JOURNAL OF MAGNETIC RESONANCE 66, 470–482 (1986)

Efficient Adiabatic Fast Passage for NMR Population Inversion in the Presence of Radiofrequency Field Inhomogeneity and Frequency Offsets

C. J. HARDY, W. A. EDELSTEIN, AND D. VATIS

General Electric Corporate Research and Development, Schenectady, New York 12301

Received August 2, 1985; revised September 22, 1985

Adiabatic fast passage is a powerful tool for uniformly inverting magnetization in the presence of rf magnetic field inhomogeneity and frequency offsets. Long pulses or large rf powers are necessary for this technique to be effective, however, when the usual linear frequency sweep is used. A sweep of the form $\omega(t) - \omega_0 = \omega_1 \tan(\alpha\omega_1 t)$, on the other hand, is shown to be an order of magnitude more efficient than the linear sweep. Here $\omega(t)$ is the rf field frequency, ω_0 is the Larmor frequency, $\omega_1 = \gamma B_1$ (gyromagnetic ratio times rf field strength), and α is a constant determined by ω_1, the total sweep time, and the range of the frequency sweep. This tangential frequency sweep can produce substantially better inversion than composite pulses of the same amplitude. © 1986 Academic Press, Inc.

Good population inversion between spin levels is important for a number of applications in NMR. It enables accurate measurement of spin–lattice relaxation time T_1 without long recovery times between cycles (*1*). It is also helpful in various spectroscopic techniques such as polarization transfer (*2*) and certain types of two-dimensional spectroscopy (*3*). Uniform inversion is not always easy to achieve, either because of spatial inhomogeneity across the sample in the rf or static magnetic fields, or because of frequency offsets between the rf field and chemically shifted spins. Adiabatic fast passage (AFP), first discovered by Bloch in the early years of NMR (*4, 5*), has proven to be an effective technique for inverting spins in the presence of such factors. His technique involves the linear sweeping of the static field or rf frequency through the spin resonance in order to rotate the magnetization down to an inverted position. Linear sweep AFP, however, requires long times or large amounts of rf power, making it undesirable for some applications.

As an alternative a family of composite pulses have been proposed which have many of the advantages of linear sweep AFP while requiring less rf power (*6–10*). In particular, the $90°(X)\ 360°(X + 2\pi/3)\ 90°(X)$ and $45°(-Y)\ 90°(X)\ 90°(Y)\ 45°(X)\ 180°(Y)\ 45°(X)\ 90°(-Y)\ 90°(X)\ 45°(Y)$ composites (*7*) have been shown to be effective in the presence of wide rf field inhomogeneity, while the $90°(X)\ 200°(Y)\ 80°(-Y)\ 200°(Y)\ 90°(X)$ composite (*8*) performs well over a wide range of rf frequency offset. The $90°(X)\ 240°(Y)\ 90°(X)$ composite (*6, 8*), $90°(Y)\ 90°(X)\ 90°(-Y)\ 180°(X)\ 90°(-Y)\ 90°(X)\ 90°(Y)$ composite (*9*), and $270°(-X)\ 360°(X)\ 90°(Y)\ 270°(-Y)\ 360°(Y)\ 90°(X)$ composite (*10*), on the other hand, have been shown to be effective both in the presence of moderate frequency offset and rf field inhomogeneity. Tycko and Pines (*11*) have

0022-2364/86 $3.00

recently produced a composite pulse which is both insensitive to a broad range of frequency offsets and large rf field inhomogeneities. This sequence, however requires 25 successive π pulses of varying phases, making it impractical in many cases.

We propose a new form of AFP which employs a tangential rather than a linear frequency sweep. This sweep follows from a more exact statement of the Bloch condition, and enables good inversion of magnetization both in the presence of rf field inhomogeneity and frequency offset, while using an order of magnitude less power than the linear sweep.

THEORY

To understand the Bloch condition, consider an AFP experiment as seen in the rotating frame (Fig. 1). The rf field $\mathbf{B}_1$ is a constant, pointing along the y axis. Since

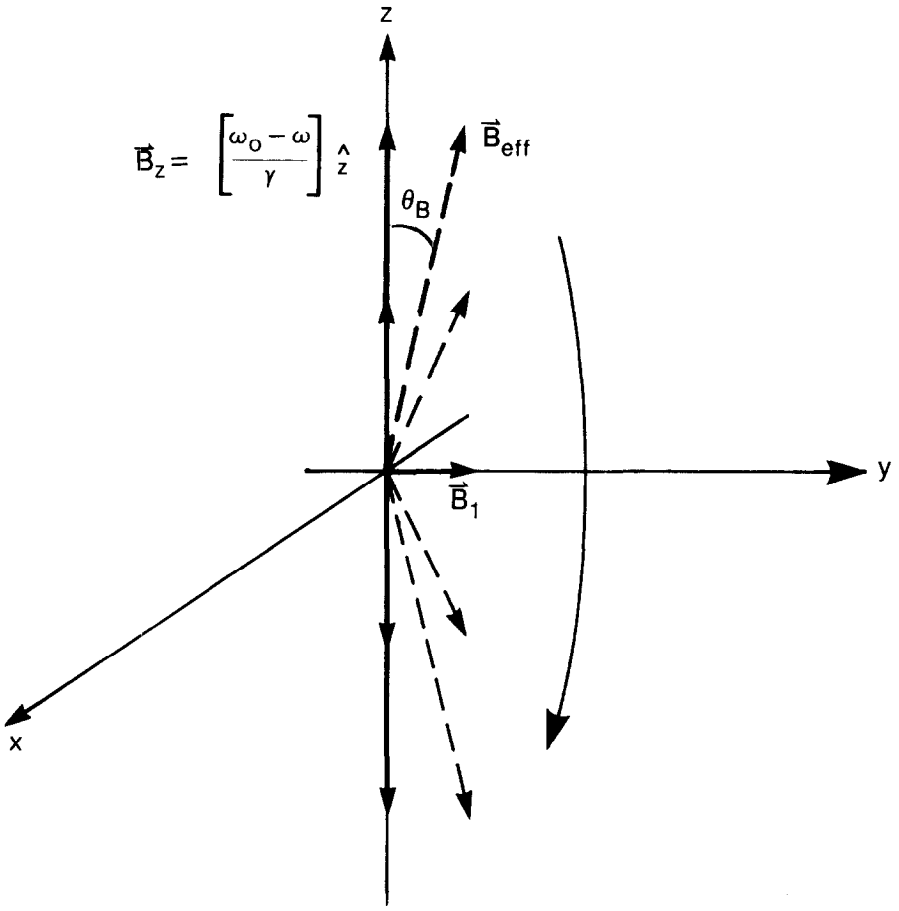

FIG. 1. AFP experiment as seen in a reference frame rotating at the Larmor frequency ω_0 about the z axis of the laboratory frame. $\mathbf{B}_1$ is constant, pointing along the y axis. $\mathbf{B}_z$ is proportional to the frequency offset, $(\omega(t) - \omega_0)$. As $\omega(t)$ is swept up through ω_0, the total effective field $\mathbf{B}_{eff}$ is swept down in an arc in the yz plane. If the sweep is slow enough, the magnetization $\mathbf{M}$ (not shown) will follow $\mathbf{B}_{eff}$ down, and be left inverted.

the rf frequency $\omega(t)$ is being swept through the Larmor frequency ω_0, then at any given time there will also be a z component of magnetic field

$$\mathbf{B}_z = [(\omega_0 - \omega)/\gamma]\hat{z}. \quad [1]$$

The total effective field $\mathbf{B}_{\text{eff}}$ at a given time is then the vector sum of $\mathbf{B}_1$ and $\mathbf{B}_z$ and points at an angle θ_B relative to the z axis. As ω is swept up through ω_0, then $\mathbf{B}_z$ shrinks down through zero to negative values, and $\mathbf{B}_{\text{eff}}$ is swept through an arc in the yz plane until it points essentially along $-z$. If the sweep is slow enough, then the magnetization, which starts out in its equilibrium position along z, follows $\mathbf{B}_{\text{eff}}$ down and is left inverted.

For $\mathbf{M}$ to keep up with $\mathbf{B}_{\text{eff}}$, the rate of precession ω_{eff} of $\mathbf{M}$ about $\mathbf{B}_{\text{eff}}$ must be faster than the angular velocity of $\mathbf{B}_{\text{eff}}$, $d\theta_B/dt$, i.e. (*12*),

$$\omega_{\text{eff}} = \gamma B_{\text{eff}} \gg \frac{d\theta_B}{dt}. \quad [2]$$

But

$$\tan \theta_B = \left[\frac{\gamma B_1}{\omega_0 - \omega}\right], \quad [3]$$

and

$$B_{\text{eff}} = (1/\gamma)\sqrt{(\omega - \omega_0)^2 + (\gamma B_1)^2}. \quad [4]$$

So

$$\frac{d\theta_B}{dt} = \frac{B_1}{\gamma B_{\text{eff}}^2}\left[\frac{d(\omega - \omega_0)}{dt}\right]. \quad [5]$$

Combining Eqs. [2] and [5], we get

$$\frac{\gamma^2 B_{\text{eff}}^3}{B_1} \gg \frac{d(\omega - \omega_0)}{dt}. \quad [6]$$

Since the minimum value of B_{eff} is B_1, Eq. [6] becomes the Bloch condition

$$\frac{d}{dt}(\omega - \omega_0) \ll \omega_1^2, \quad [7]$$

where $\omega_1 = \gamma B_1$. The lower limit on the sweep rate is determined by the requirement that no decay of transverse magnetization occur during a period of nutation, and yields

$$\frac{\omega_1}{T_2} \ll \left|\frac{d}{dt}(\omega - \omega_0)\right| \ll \omega_1^2, \quad [8]$$

where T_2 is the spin–spin relaxation time.

Linear frequency sweeps determined by Eq. [8] require relatively large amounts of rf power to invert the magnetization completely. This is because by substituting B_1 into B_{eff} in Eq. [6], we have made the upper limit on the sweep rate more restrictive than it needs to be for all points in the sweep. Since ω_{eff} is much larger at the beginning and end of the sweep than in the middle, $d\theta_B/dt$ can be increased there accordingly. To do this, we rewrite Eq. [6] as

$$\alpha \frac{\gamma^2 B_{\text{eff}}^3}{B_1} = \frac{d}{dt}(\omega - \omega_0), \qquad [9]$$

where $0 < \alpha < 1$. Substituting from Eq. [4] and solving for $\omega(t)$, we find

$$\omega(t) - \omega_0 = \omega_1 \left[\frac{\alpha \omega_1 t}{\sqrt{1 - (\alpha \omega_1 t)^2}} \right]. \qquad [10]$$

This sweep has been found to invert magnetization much more efficiently than a linear one (*13*).

By formulating the Bloch condition in a slightly different manner from Eq. [2], we can obtain an even better sweep function than Eq. [10]. If we require that **M** precess about $\mathbf{B}_{\text{eff}}$ at a faster rate than the change in $\mathbf{B}_z$, then

$$\alpha \omega_{\text{eff}}^2 = \left[\frac{d}{dt}(\omega - \omega_0) \right], \qquad [11]$$

where $0 < \alpha < 1$. Substituting from Eq. [4] and rearranging yields

$$\alpha \int_0^t dt = \int_0^{\omega - \omega_0} [(\omega - \omega_0)^2 + (\gamma B_1)^2]^{-1} d(\omega - \omega_0). \qquad [12]$$

Integrating and again rearranging, we obtain a tangential sweep

$$\omega(t) - \omega_0 = \omega_1 \tan(\alpha \omega_1 t), \qquad [13]$$

where $-T_0/2 \leq t \leq T_0/2$, T_0 being the total sweep time. This function is illustrated in Fig. 2, along with a linear sweep. The constant α is determined by ω_1, T_0, and the range of the angular frequency sweep 2Ω:

$$\alpha = \left[\frac{2}{\omega_1 T_0} \right] \arctan \left[\frac{\Omega}{\omega_1} \right]. \qquad [14]$$

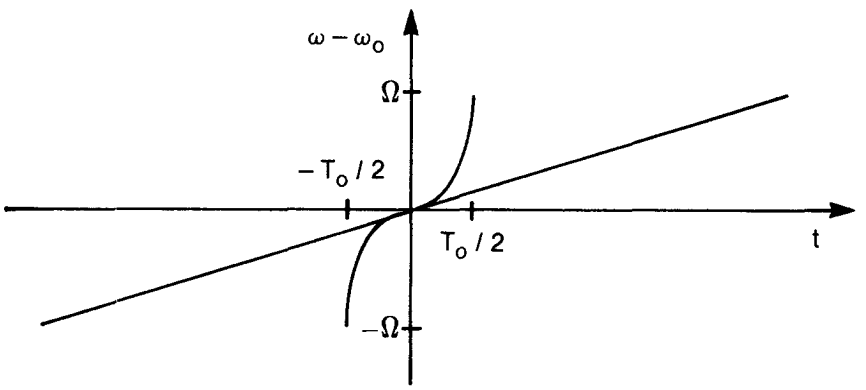

FIG. 2. Tangential and linear frequency sweeps. The tangential sweep changes quickly at the beginning and end and slowly in the middle, where $\mathbf{B}_{\text{eff}}$ is small.

As an example, if $B_1 = 0.235$ G, (corresponding to a simple π pulse time of 500 μs for hydrogen) then a 2 ms sweep from 20 kHz below resonance to 20 kHz above resonance would use $\alpha = 0.242$.

An interesting feature of the tangential sweep is that the angle θ_B between $\mathbf{B}_{eff}$ and the z axis changes linearly in time, as does the angle θ_M between $\mathbf{M}$ and the z axis. Combining Eqs. [3] and [13], we have

$$\theta_B = \alpha\omega_1 t + \frac{\pi}{2}. \qquad [15]$$

As $\mathbf{B}_{eff}$ rotates down in the yz plane, $\mathbf{M}$ is swept down parallel to $\mathbf{B}_{eff}$, essentially in a vertical plane located at an angle $\epsilon = \alpha$ relative to the yz plane (Fig. 3). $\mathbf{M}$ makes minor oscillations in and out of this plane during the course of the sweep, but the angle θ_M of $\mathbf{M}$ with respect to the z axis at any given time is always the same as θ_B. Figure 4a shows $\theta_B(t)$, $\theta_M(t)$, and $\epsilon(t)$ for a 2 ms tangential sweep from -50 to $+50$ kHz through resonance, with $B_1 = 0.235$ G. Figure 4b shows these same functions for one particular linear sweep (to be described in more detail later). These curves are computer simulations obtained by numerical solution of the Bloch equations.

There are two ways one may implement the tangential sweep in practice. The first is to incorporate frequency-sweeping capability directly into the spectrometer. In our

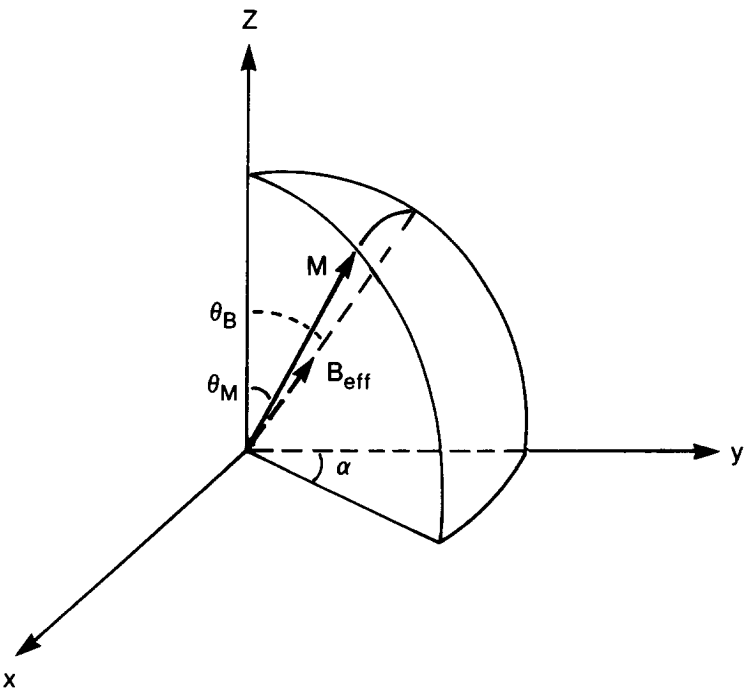

FIG. 3. Effective field $\mathbf{B}_{eff}$ and magnetization $\mathbf{M}$ part way through AFP, for the case of a tangential frequency sweep. The angle $\theta_B(t)$ increases linearly in time as $\mathbf{B}_{eff}$ sweeps down in the yz plane. The magnetization $\mathbf{M}$ rotates down parallel to $\mathbf{B}_{eff}$ essentially in a vertical plane located at an angle $\epsilon = \alpha$ relative to the yz plane, where α is given by Eq. [14]. Only one quadrant is shown, for clarity.

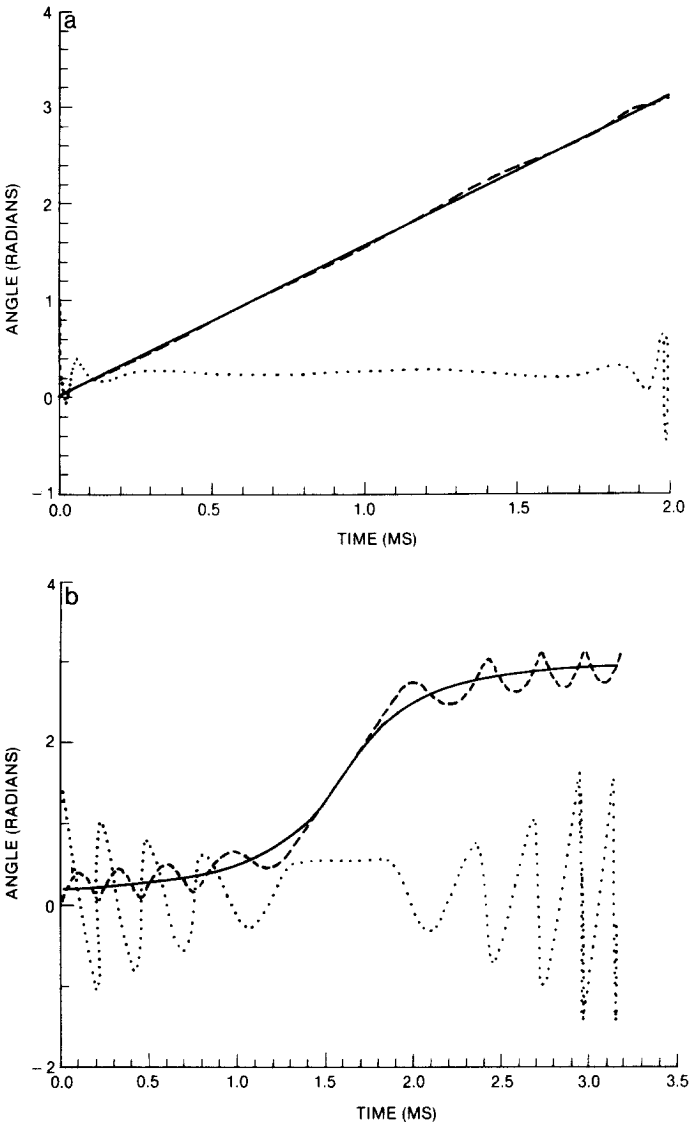

FIG. 4. (a) Angles $\theta_B(t)$ (solid line), $\theta_M(t)$ (dashed line), and $\epsilon(t)$ (dotted line) for a $\pm$ 50 kHz, 2 ms tangential sweep with $B_1 = 0.235$ G. $\theta_B(t)$ and $\theta_M(t)$ are linear in time, extending from 0 to π. To first approximation $\epsilon(t) = \alpha$. The deviations of **M** at the beginning and end of the sweep from the plane located at $\epsilon = \alpha$ are actually fairly small since the magnetization is almost vertical at these points. (b) Angles $\theta_B(t)$ (solid line), $\theta_M(t)$ (dashed line), and $\epsilon(t)$ (dotted line) for a $\pm$ 5 kHz, 3.2 ms linear sweep with $B_1 = 0.235$ G. **M** precesses many times about $\mathbf{B}_{\text{eff}}$ during the course of the sweep, resulting in oscillations in $\theta_M(t)$ and $\epsilon(t)$.

case this is done by use of a 10 MHz voltage-controlled oscillator (VCO) which is mixed up to the hydrogen Larmor frequency at 62 MHz (*13*). A tangential voltage ramp into the VCO then produces a tangential frequency sweep through the proton resonance.

If, on the other hand, one has a single-sideband quadrature transmitter with the capability to generate arbitrary waveforms, one may use frequency modulation to produce the frequency sweep. Integrating Eq. [13] gives the phase angle as a function of time for the tangential sweep:

$$\phi(t) = \omega_0 t - \left[\frac{1}{\alpha}\right]\ln(\cos(\alpha\omega_1 t)). \quad [16]$$

The modulating waveforms for the two transmitter channels I and Q then become

$$I(t) = \cos\left[\frac{1}{\alpha}\ln(\cos(\alpha\omega_1 t))\right] \quad [17]$$

$$Q(t) = -\sin\left[\frac{1}{\alpha}\ln(\cos(\alpha\omega_1 t))\right]. \quad [18]$$

Figure 5 plots these functions for a ±50 kHz, 2 ms, 0.235 G sweep. Modulating functions of N points will provide the resolution necessary to go as high as $\Omega T_0 \sim N\pi$ without much distortion from undersampling.

RESULTS

That the tangential sweep is more efficient than the linear sweep can be seen from Figs. 6 and 7. Figures 6a and b are computer simulations of the final z magnetization after AFP versus the rf field strength times the total sweep time, for linear sweeps with six different values of (Ω/ω_1). The quantity (Ω/ω_1) defines the starting and ending

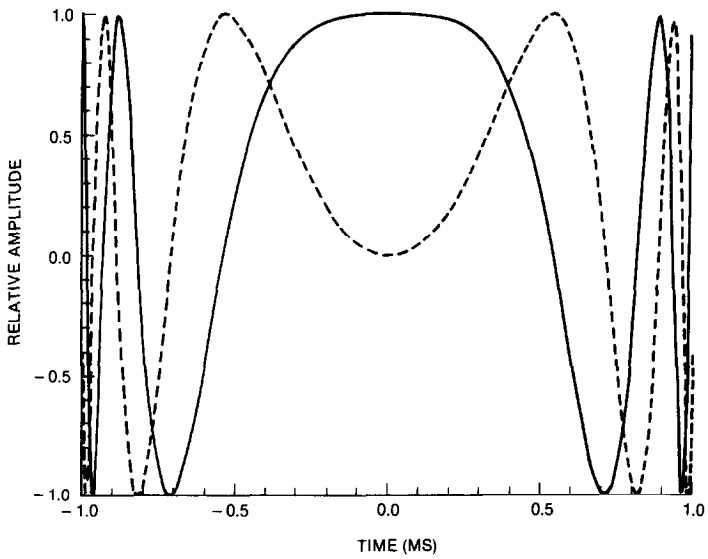

FIG. 5. I (solid line) and Q (dashed line) waveforms for frequency modulation corresponding to a ± 50 kHz, 2 ms, 0.235 G tangential frequency sweep.

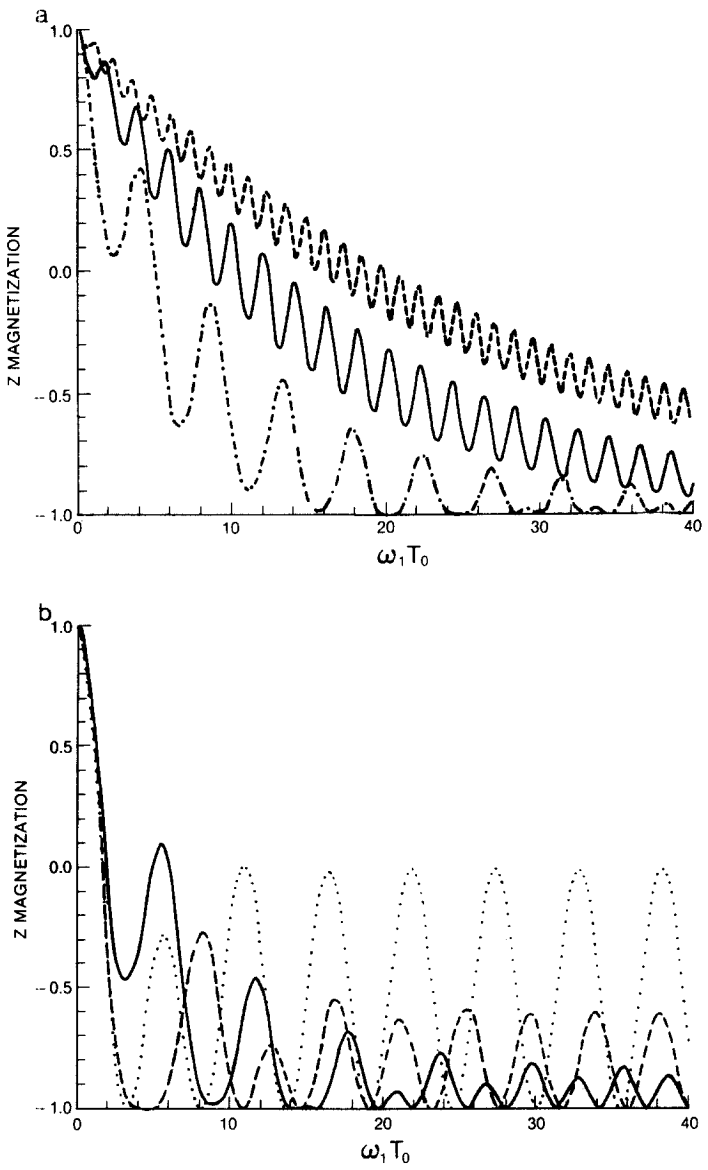

FIG. 6. Final z magnetization after linear AFP versus rf field strength times total sweep time, for six different values of (Ω/ω_1). (a) Dashed line 20; solid line 12; dash–dot line 5. (b) Solid line 3.5; dashed line 2; dotted line 1. The linear sweep of Fig. 4b corresponds to an abscissa of 20 on the dash–dot curve of part (a).

values of the sweep angle θ_B. Figure 7 shows the same thing for a tangential sweep with $(\Omega/\omega_1) = 50$. For reference, a simple π pulse would lie at $\omega_1 T_0 = \pi$ on the graph. It is evident that while it is possible with the linear sweep to achieve complete inversion at an abscissa approaching π, the exact value of $\omega_1 T_0$ then becomes critical. Correspondingly, the inversion of magnetization becomes very sensitive to B_1 amplitude

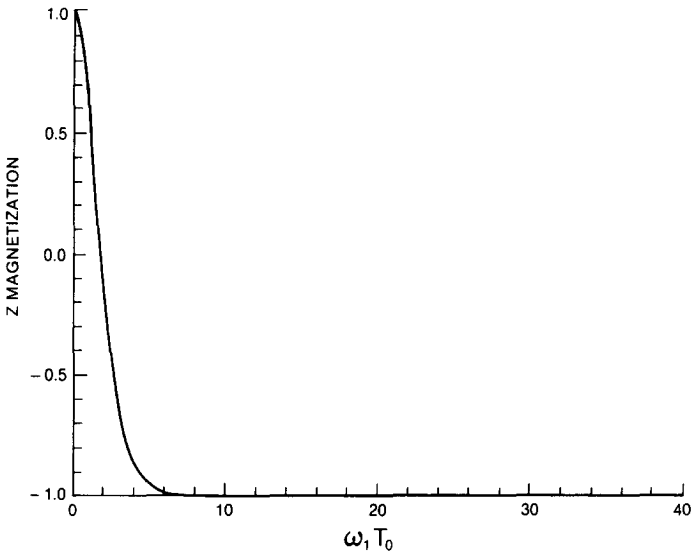

FIG. 7. Final z magnetization after tangential AFP versus rf field strength times total sweep time, for $(\Omega/\omega_1) = 50$. All curves with $(\Omega/\omega_1) \geq 20$ look roughly the same in this region of $\omega_1 T_0$, while curves with lower (Ω/ω_1) start to exhibit oscillation.

and frequency offset, nullifying the original reason for using AFP. For the linear sweep one would have to move out to an abscissa of ~ 150 to achieve complete inversion in the presence of such factors. For the tangential sweep of Fig. 7, on the other hand, good inversion is achieved over a wide range of $\omega_1 T_0$, starting at $\sim 2\pi$. All values of $(\Omega/\omega_1) \geq 20$ produce virtually identical curves (in this range of $\omega_1 T_0$) while smaller sweep ranges tend to produce oscillations similar to the dotted curve in Fig. 6b.

AFP with a tangential frequency sweep shows excellent insensitivity to rf inhomogeneity. This can be seen from the dashed line in Fig. 8, which plots final z magnetization after the pulse versus the ratio of rf field strength to its nominal value. For this curve $\omega_1 T_0 = 18$ and $(\Omega/\omega_1) = 50$. The same quantity is plotted for a simple π pulse, a $90°(X)\,240°(Y)\,90°(X)$ composite (*7*), and a $90°(X)\,200°(Y)\,80°(-Y)\,200°(Y)\,90°(X)$ composite (*8*) for comparison. (This last pulse has been proposed for its immunity to rf frequency offsets, not rf inhomogeneity.) It can be seen that if one drives the AFP pulse at $\sim 1.5 B_1^0$ then B_1 errors as high as $\pm 60\%$ will produce negligible effect on the inversion. In this case the AFP pulse will be roughy twice as long as the five pulse composite, assuming the same rf field strength is used for both pulses.

The AFP pulse with tangential sweep is likewise insensitive to rf frequency offset. Figure 9 shows the z magnetization after the pulse versus frequency offset, for this pulse as well as for the simple π pulse and the two composites mentioned above. The AFP curve remains flat out to $\Delta\omega/\omega_1 = \pm 1$. For $B_1 = 0.235$ G and $B_0 = 1.5$ T, this corresponds to ± 16 ppm in the hydrogen spectrum, which will easily accommodate most spectra of interest.

To test these simulations, experiments were performed on a small vial of agarose–$CuSO_4$, using a General Electric 1.5 T whole-body research system. An inversion–

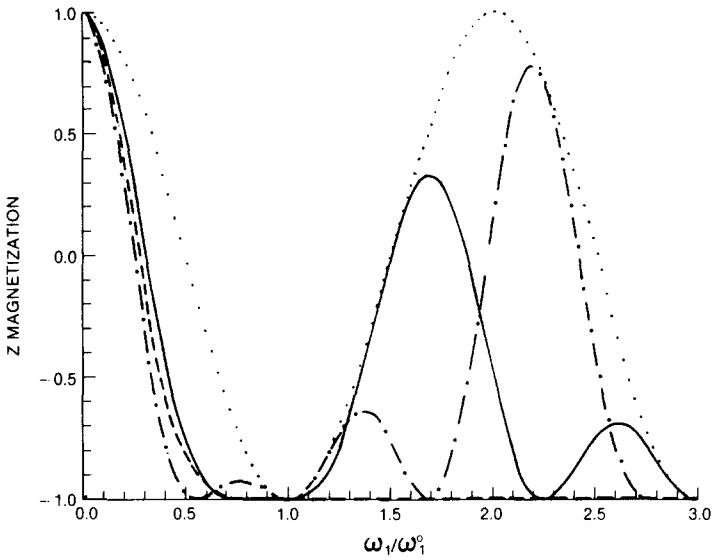

FIG. 8. Final z magnetization after pulse versus ratio of rf field strength to its nominal value, for four different pulses. Dotted line, simple π pulse; dashed line, tangential AFP of the form $\omega(t) - \omega_0 = \omega_1^0 \tan(\alpha\omega_1^0 t)$, with $(\Omega/\omega_1^0) = 50$, $\omega_1^0 T_0 = 18$; solid line, $90°(X)\ 240°(Y)\ 90°(X)$ composite; dash–dot line, $90°(X)\ 200°(Y)\ 80°(-Y)\ 200°(Y)\ 90°(X)$ composite. An AFP pulse driven at $\omega_1 = 1.5\ \omega_1^0$ produces complete inversion over a wide range of ω_1.

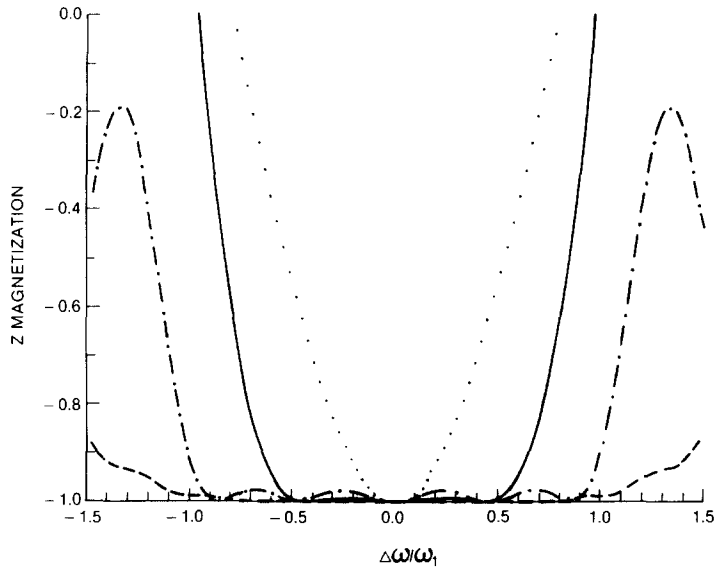

FIG. 9. Final z magnetization after pulse versus normalized resonance offset $\Delta\omega/\omega_1$, for four different pulses. Dotted line, simple π pulse; dashed line, tangential AFP of the form $\omega(t) - \omega_0 = \omega_1^0 \tan(\alpha\omega_1^0 t)$, with $(\Omega/\omega_1^0) = 50$, $\omega_1^0 T_0 = 18$, and $\omega_1 = 1.5\ \omega_1^0$; solid line, $90°(X)\ 240°(Y)\ 90°(X)$ composite; dash–dot line, $90°(X)\ 200°(Y)\ 80°(-Y)\ 200°(Y)\ 90°(X)$ composite. Tangential AFP produces complete inversion over a range $\Delta\omega = \pm\omega_1$.

recovery pulse sequence was run, with the magnetization "read out" immediately after inversion, and with a recovery time which was long compared to T_1. A tangential frequency sweep from −20 to +20 kHz through resonance was used for the inverting pulse, with B_1 = 0.235 G. The results for various sweep times are displayed as the data points in Fig. 10, which show good agreement with the theoretical curve (solid line). To model the effect of B_1 errors the same pulse sequence was run with the height of the inverting pulse varied. Figure 11 shows the results for AFP and the simple π pulse. The nominal B_1 = 0.235 G here. Again there is good agreement with the theoretical curves, shown by the solid and dotted lines.

To model the effect of frequency offset, a variable dc voltage offset was added to the tangential voltage ramp into the VCO. For the simple π pulse, the tangential ramp was replaced with a variable dc voltage at the VCO input. A dc level of 460 mV corresponds to an offset of 30 ppm in our spectrometer. The results are shown as the data points in Fig. 12. Again there is good agreement with theory, represented by the curves in the same figure.

DISCUSSION

AFP with a tangential frequency sweep has been shown to produce good inversion both in the presence of B_1 spatial inhomogeneity and of resonance frequency offsets. A major problem with composite pulses is (*8*) that one has not yet been found which is insensitive to both large B_1 inhomogeneity and frequency offsets while being of reasonable duration. On the other hand, linear sweep AFP has also suffered from its relatively long duration and concomitant large rf powers. Use of a tangential frequency

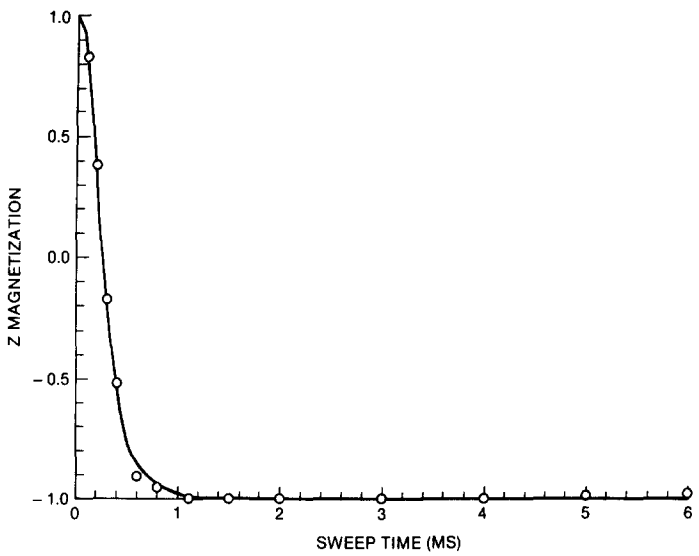

FIG. 10. Final z magnetization versus total sweep time for a ± 20 kHz tangential frequency sweep with B_1 = 0.235 G. The data points are the results of an inversion–recovery pulse sequence with short inversion time and long recovery time, performed on a vial of agarose–$CuSO_4$. The data show good agreement with the corresponding computer simulation, drawn as a solid line.

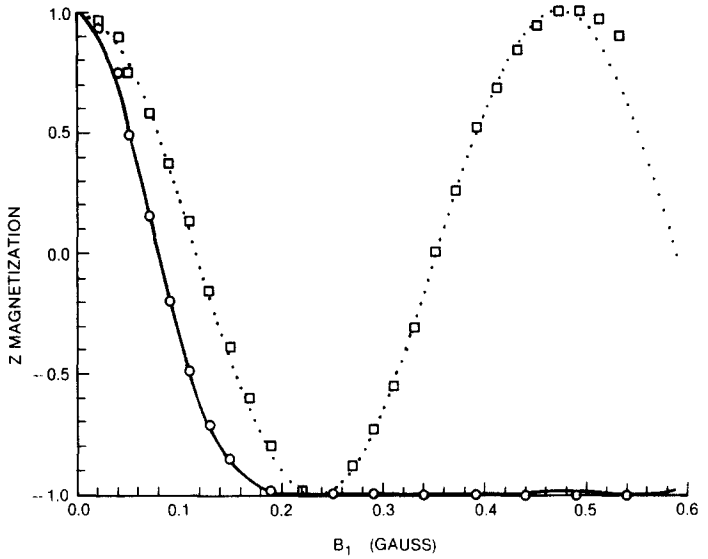

FIG. 11. Final z magnetization after pulse versus B_1, for a simple π pulse (dotted line and boxes) and for ±20 kHz, 2 ms tangential AFP (solid line and circles). The nominal rf field $B_1^0 = 0.235$ G here. The data were obtained in the same way as for Fig. 10, only varying the height of the inverting pulse rather than the sweep time. There is again good agreement with the corresponding computer simulations, shown as the lines in the figure.

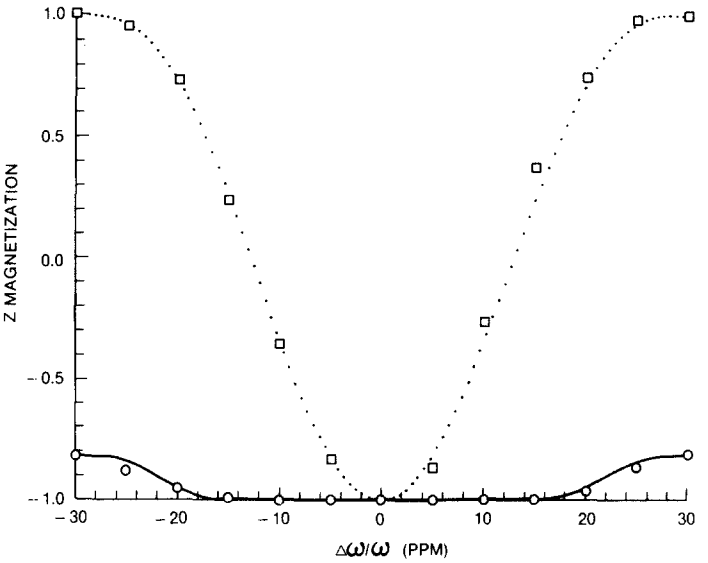

FIG. 12. Final z magnetization after pulse versus frequency offset (in ppm), for the simple π pulse (dotted line and boxes) and for ±20 kHz, 2 ms tangential AFP driven at $1.5 \times 0.235 = 0.353$ G (solid line and circles). The data are again from an inversion–recovery experiment on a vial of agarose–$CuSO_4$. For the circular data points the frequency offset was created by adding a dc voltage to the tangential voltage ramp into the VCO. For the squares the offset was produced by feeding a dc voltage into the VCO input. The lines are the corresponding computer simulations.

sweep goes a long way toward solving this problem. In fact, AFP with a tangential sweep can produce results comparable to the linear sweep while taking an order of magnitude less time, although it is still somewhat longer than the simpler composite pulses. While AFP is at present more difficult to implement in conventional spectrometers than the composite pulses, in many cases frequency sweeping capability can easily be incorporated directly into the spectrometer through use of a VCO or similar circuit, or can be implemented through the equivalent frequency modulation.

The modified AFP should prove promising for medical applications, where B_1 and B_0 inhomogeneity may be more important factors than in high-field spectroscopy. Complete inversion of magnetization in the presence of such factors would allow accurate measurement of T_1 without long recovery times between cycles. *In vivo* spectroscopic techniques requiring broadband inversion would also benefit from this tool. In addition, the tangential frequency sweep would drastically reduce the rf power deposited in the patient, which is especially important at higher fields. Medical NMR imagers are often equipped with frequency sweeping capability. We have successfully implemented the tangential AFP in our research system using both the VCO technique and the quadrature FM technique.

ACKNOWLEDGMENT

We thank W. J. Adams for writing the inversion–recovery pulse sequence for acquisition of the data in Figs. 10, 11, and 12.

REFERENCES

1. D. CANET, G. C. LEVY, AND I. R. PEAT, *J. Magn. Reson.* **18,** 199 (1975).
2. G. A. MORRIS AND R. FREEMAN, *J. Am. Chem. Soc.* **101,** 760 (1979).
3. A. BAX, "Two-Dimensional Nuclear Magnetic Resonance in Liquids," Delft Univ. Press (D. Reidel), Dordrecht, 1982.
4. F. BLOCH, *Phys. Rev.* **70,** 460 (1946).
5. F. BLOCH, W. W. HANSEN, AND M. PACKARD, *Phys. Rev.* **70,** 474 (1946).
6. R. FREEMAN, S. P. KEMPSELL, AND M. H. LEVITT, *J. Magn. Reson.* **38,** 453 (1980).
7. M. H. LEVITT, *J. Magn. Reson.* **48,** 234 (1982).
8. M. H. LEVITT, *J. Magn. Reson.* **50,** 95 (1982).
9. M. H. LEVITT AND R. R. ERNST, *J. Magn. Reson.* **55,** 247 (1983).
10. A. J. SHAKA AND R. FREEMAN, *J. Magn. Reson.* **55,** 487 (1983).
11. R. TYCKO AND A. PINES, *Chem. Phys. Lett.* **111,** 462 (1984).
12. J. G. POWLES, *Proc. Phys. Soc. London* **71,** 497 (1958).
13. C. J. HARDY, W. A. EDELSTEIN, D. VATIS, R. HARMS, AND W. J. ADAMS, *Magn. Reson. Imag.* **3,** 107 (1985).